Research Paper
Computational Methods for Differential Equations
http://cmde.tabrizu.ac.ir
Vol. *, No. *, *, pp. 1-19
DOI:10.22034/cmde.2024.58127.2451

Analysis of the effect of isolation on the transmission dynamics of COVID-19: a mathematical modelling approach (R1)

Abayomi Ayotunde Ayoade[1,*], **Oluwatayo Micheal Ogunmiloro**[2], **and Oyedepo Taiye**[3]

[1]Department of Mathematics, University of Lagos, Lagos, Lagos State, Nigeria.

[2]Department of Mathematics, Ekiti State University, Ado-Ekiti, Ekiti State, Nigeria.

[3]Department of Applied Sciences, Federal College of Dental Technology and Therapy, Enugu, Enugu State, Nigeria.

Abstract

COVID-19 was declared a pandemic on March 11, 2020, after the global cases and mortalities in more than 100 countries surpassed 100 000 and 3 000, respectively. Because of the role of isolation in disease spread and transmission, a system of differential equations was developed to analyse the effect of isolation on the dynamics of COVID-19. The validity of the model was confirmed by establishing the positivity and boundedness of its solutions. Equilibria analysis was conducted, and both zero and nonzero equilibria were obtained. The effective and basic reproductive ratios were also derived and used to analyse the stability of the equilibria. The disease-free equilibrium is stable both locally and globally if the reproduction number is less than one; otherwise, it is the disease-endemic equilibrium that is stable locally and globally. A numerical simulation was carried out to justify the theoretical results and to visualise the effects of various parameters on the dynamics of the disease. Results from the simulations indicated that COVID-19 incidence and prevalence depended majorly on the effective contact rate and per capita probability of detecting infection at the asymptomatic stage, respectively. The policy implication of the result is that disease surveillance and adequate testing are important to combat pandemics.

Keywords. Pandemic, Reproductive ratio, Simulation, Parameters, Incidence, Prevalence.

2010 Mathematics Subject Classification. 92B05; 34D08; 34D20; 34D23.

1. Introduction

A fatal viral eruption known as coronavirus disease 2019 (COVID-19), formerly called 2019- novel coronavirus (2019-nCoV) ushered in the year 2020. The disease, which is instigated by SARS-CoV-2, appeared from Wuhan, the commercial hub and capital of Hubei, China towards the end of December 2019 [34]. Within short time, COVID-19 invaded China leading to upsurge in reported cases and mortalities. The World Health Organisation (WHO) declared COVID-19 a pandemic on March 11, 2020, having infected over 118,000 and claimed almost 4,300 lives in more than 100 countries worldwide [12]. The pandemic spread to more than 210 countries and established itself a major burden to health system and economies across the globe [20]. In less than a year precisely on 1st October 2020 (10:31 GMT), the confirmed cases and mortalities of COVID-19 rose to 34,192,734 and 1,019,242 respectively worldwide [4].

Symptoms and signs for COVID-19 usually develop within two weeks. When the symptoms are fully developed, infected individuals may exhibits cough, fever or respiratory syndromes such as breathing disorders and shortness of breaths [47]. Infected individuals with acute symptoms may manifest acute respiratory distress syndrome (ARDs) or worse-respiratory track disorders, such as bronchitis and pneumonia. These difficulties are more noticeable in infants and the elderly as well as individuals with comorbidities or underlying health challenges such as immune-compromised patients and cardiopulmonary disorders [10]. Effective and safe vaccines against COVID-19 infections in humans were not in existence at the start of the outbreak. As a result, the mitigation and control measures against the spread of the disease were based on employing non-pharmaceutical measures, such as contact tracing, social distancing, community

Received: 24 August 2023; Accepted: 27 March 2024.
∗ Corresponding author. Email: ayoadeabbayomi@gmail.com; ayoayoade@unilag.edu.ng .

lockdown, quarantine, isolation and face masks usage in public [16, 32]. Social distancing is about keeping 2 meters distance from individuals in public gatherings. Community lockdown involves applying the closure of non-vital services and businesses and schools, preventing large gatherings and enforcing the stay-at-home [20].

Mathematical models have become important tools for providing insights into the dynamics of contagious diseases, right from 1900s when the groundbreaking works of Ross and Kermack-McKendrick appeared [5, 15, 24, 33, 35–37]. Interestingly, numerous studies have contributed to the investigation of dynamics and control of COVID-19 in several human populations. [17] formulated an agent-based model for COVID-19 to evaluate the effect of non-pharmaceutical interventions (NPIs) on COVID-19 deaths. The model was among the early COVID-19 models and the results of the study suggested an increasingly-high estimate for the aggregate deaths in the United States (2.2 million mortalities) and the United Kingdom (510 000 mortalities) if no interventions are implemented. A study conducted in [16] adopted a multi-group epidemic model of Kermack-Mckendrick type to examine the effect of masks usage in checking COVID-19 transmission in the US. Their work indicates that face masks usage is of high benefit in reducing community spread of the pandemic. The study however reveals that the community-wide impact of face masks usage depends on the general compliance as well as the applications of other NPIs (such as contact tracing, social distancing, etc.).

A model for evaluating the effect of NPIs on mitigating and checking the spread of COVID-19 was formulated by [32]. Their study reveals that a second outbreak of COVID-19 is possible if enforcement and applications of NPIs (contact tracing, face masks usage, lockdown, social distancing etc.) are relaxed early. The researchers therefore advocate for the extension of the period of NPIs to significantly minimise the mortality of COVID-19 in the US. The dynamics of COVID-19 in Wuhan city for the months of January and February 2020 was investigated by [26] via a stochastic model. It was revealed that implementations of strict travel restrictions could instigate massive reduction in COVID-19 spread and transmission across Chinese provinces. The mechanisms of COVID-19 in other countries have also been a subject of intense mathematical studies [2, 3, 21, 25, 31, 39]. For instance, the impact of non-pharmaceutical interventions on the spread of COVID-19 was examined in Saudi Arabia in [1] and in South Afirca in [29]. Recent studies on the impact of non-pharmaceutical interventions on the spread of COVID-19 could also be accessed in [22, 30, 46].

Isolation and quarantine are two epidemiological terms that are closely related but have different interpretations. Isolation takes place when individuals who have been infected with a disease whether asymptomatically or symptomatically are confined to a close space to prevent further infections. Quarantine, on the other hand, occurs when individuals who are thought to have been exposed to a disease are confined to a close space and placed under close watch to see whether they progress to become infectious or not. Individuals who are found to be infectious during quarantine or at the end of quarantine do progress to isolation. Isolation is usually come about through testing but quarantine is achieved through contact tracing or from arrivals of people from other territories. The main distinction between isolation and quarantine is that while treatment is introduced to individuals in isolation immediately, treatment becomes necessary only if individuals in quarantine turn out to be infectious. Furthermore, while suspected cases of infections go to quarantine, confirmed cases progress to isolation.

Apart from the work of [19] where a stochastic model was used to examine the dynamics of COVID-19 and where the result of the study affirmed the possibility of eradicating COVID-19 in a population within 3 months if effective contact tracing and isolation policies are implemented, studies on the effect of isolation on the dynamics of COVID-19 are rare in the literature especially with the use of a mathematical model. It is on this ground that this work is motivated to use a mathematical modelling approach to analyse the effect of isolation on the transmission of COVID-19. Besides, although COVID-19 is gradually dying off at present, and some countries have started relaxing mitigation measures, while other countries have completely relaxed all measures, this study would provide important information about isolation strategy to adequately equip various communities towards future outbreak of infectious diseases.

2. Model Formulation and Basic Properties

The sum of the population at any given time t, represented by $N(t)$, is split into sub-populations comprising susceptible individuals $S(t)$ (people who are at the risk of infection), exposed individuals $E(t)$ (people who carry the pathogen without exhibiting any clinical signs but can spread the virus), infected individuals $I(t)$ (people who carry the virus, manifest the symptoms and are more contagious), treatment class $T(t)$ (consists of individuals who have

been isolated whether before they are symptomatic $E(t)$ or after they are symptomatic $I(t)$ and placed in a close space for treatment) and recovered individuals $R(t)$ (people who have been treated and cured of the disease). Our model mimics the reality that during the hot period of COVID-19, individuals were encouraged to undergo COVID-19 test and through the exercise, many asymptomatic individuals were discovered and isolated for treatment. This method played a significant role and altered the dynamics of COVID-19 in many part of the world. It is also assumed that individuals in the compartment $R(t)$ remains in the compartment throughout the analysis and do not contract the virus again. The flow between the compartments of the model is displayed in Figure 1.

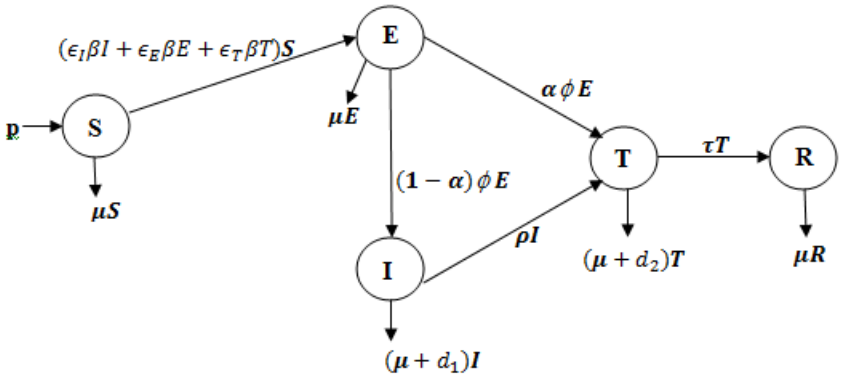

FIGURE 1. The model transfer diagram.

The total population $N(t)$ is given by

$$N(t) = S(t) + E(t) + I(t) + T(t) + R(t) \tag{2.1}$$

The influx into the population either by births or from other territories is denoted by p, and the mortality rate unrelated to COVID-19 in all compartments is denoted by μ (day^{-1}). The per capita probabilities that a susceptible contract the virus from a symptomatic infected individual, an asymptomatic infected individual and an isolated infected individual are $\epsilon_I\beta$ (day^{-1}), $\epsilon_E\beta$ (day^{-1}) and $\epsilon_T\beta$ (day^{-1}) respectively, where ϵ_I, ϵ_E and ϵ_T are the parameters that are reducing the rates of infection. Since disease transmission is usually not linear [8], parameters ϵ_I, ϵ_E and ϵ_T denote various protective measures (e.g. lockdown, social distancing, handwashing, use of face masks, environmental sanitation, etc.) that affect disease transmission. The proportion α (day^{-1}) of the asymptomatic infectious individuals who are detected through testing are isolated for treatment at rate ϕ while the remaining individuals $(1-\alpha)$ (day^{-1}) move to the symptomatic infectious class at the same rate ϕ. Mortality due to COVID-19 is assumed nonexistence at the asymptomatic infectious phase. The parameters d_1 and d_2, measured *per day*, denote COVID-19- mortality rates in the symptomatic and treatment compartments, respectively. ρ (day^{-1}) is the rate of moving symptomatic infected individuals into the treatment class while τ (day^{-1}) is the recovery rate. Following the assumptions, notations and the compartmental structure of Figure 1, the following equations are derived for COVID-19 dynamics.

$$\frac{dS}{dt} = p - (\epsilon_I\beta I + \epsilon_E\beta E + \epsilon_T\beta T)S - \mu S, \tag{2.2}$$

$$\frac{dE}{dt} = (\epsilon_I\beta I + \epsilon_E\beta E + \epsilon_T\beta T)S - (\mu + \phi)E, \tag{2.3}$$

$$\frac{dI}{dt} = (1-\alpha)\phi E - (\mu + \rho + d_1)I, \tag{2.4}$$

$$\frac{dT}{dt} = \alpha\phi E + \rho I - (\mu + \tau + d_2)T, \tag{2.5}$$

$$\frac{dR}{dt} = \tau T - \mu R. \tag{2.6}$$

The initial conditions for the system are

$$S(0) = S_0, E(0) = E_0, I(0) = I_0, T(0) = T_0, R(0) = R_0. \tag{2.7}$$

Notice that $S_0 > 0$ is the total population before COVID-19 outbreak, and E_0, I_0, T_0 and R_0 are the positive initial human populations. Generally, it is assumed that $S_0 = N(0) > 0$, for which there exists only susceptible at the beginning of the epidemic while other human populations disappear. However, positive initial populations are allowed for all the variables for generality sake and, further, $N(0) = S_0 + E_0 + I_0 + T_0 + R_0$ such that Eq.(2.1) is valid at $t = 0$. A brief description of the system parameters is provided in Table 1.

COVID-19 has an incubation period of 2-14 days [11, 28]. Given the natural mortality rate μ and a life expectancy period of 70 years then $\mu = 0.000039$ per day. When COVID-19 does not exist, the population $N = \frac{p}{\mu} = 7$ million and $p = 273$. This implies that 273 susceptible individuals are added to the population per day. The influx p consists of births and net migration from the outside. The remaining values for the parameters, which are a set of logical data mostly from [4], are displayed in Table 1. Lastly, the total mortalities due to COVID-19 were derivable in the expression

$$D(t) = \int_0^t (d_1 I(\eta) + d_2 T(\eta)) d\eta, \tag{2.8}$$

subject to the initial condition $D(0) = 0$.

TABLE 1. Symbols, definitions and values for system parameters.

parameters	definitions	values
p	human recruitment rate	273 day^{-1}
β	effective contact rate	0.422 day^{-1}
ϵ_I	reduction factor in the spreading rate of infections by $I(t)$	0.3996
ϵ_E	reduction factor in the spreading rate of infections by $E(t)$	0.1899
ϵ_T	reduction factor in the spreading rate of infections by $T(t)$	0.1193
α	proportion of the infective who are detected and isolated for treatment at asymptomatic phase	0.1501 day^{-1}
ϕ	progression rate from asymptomatic phase	0.212 day^{-1}
ρ	isolation rate of symptomatic infected individuals into treatment class	0.1702 day^{-1}
τ	successful rate of treatment	0.0475 day^{-1}
d_1	COVID-19 induced mortality for symptomatic infected individuals	0.0294 day^{-1}
d_2	COVID-19 induced mortality for individuals under treatment	0.0227 day^{-1}
μ	mortality rate unrelated to COVID-19	0.000039 day^{-1}

2.1. **Boundedness and positivity of solutions.**

Boundedness of solutions. The model is biologically and mathematically meaningful in the region

$$\Omega = \left\{ (S, E, I, T, R) \in R_+^5 : N \leq \frac{p}{\mu} \right\}.$$

It is to be established that the solutions of the model that initiate in the region Ω remain in Ω and are bounded in Ω. From Eq.(2.1)

$$N(t) = S(t) + E(t) + I(t) + T(t) + R(t).$$

Obtaining the rate of change in the total population N w.r.t t by summing up Eqs. (2.2)-(2.6) then,

$$\begin{aligned} \frac{dN}{dt} &= p - \mu(S(t) + I(t) + I(t) + R(t)) - \phi E - (d_1 + d_2) I, \\ &\leq p - \mu N(t). \end{aligned} \tag{2.9}$$

$\frac{dN}{dt}$ is clearly bounded by $p - \mu N(t)$. Following standard comparison theorem applied in [6],

$$0 \leq N(t) \leq \frac{p}{\mu} + \left(N_0 - \frac{p}{\mu}\right) e^{-\mu t} \tag{2.10}$$

As $t \to \infty$, the population converges and $N \to \frac{p}{\mu}$ which indicates that $0 \leq N(t) \leq \frac{p}{\mu}$. Therefore, the feasible set of solutions for the system remains in Ω. Hence, the model is well posed and the dynamics of the disease can be sufficiently studied in Ω.

Nonnegativity of solutions. It is also of equal importance to show that aside being bounded; the solutions of the model remain nonnegative for all $t > 0$. The proof is established by the following lemmas.

Lemma 1. *if* $S(0) \geq 0$, $E(0) \geq 0$, $I(0) \geq 0$, $T(0) \geq 0$ *and* $R(0) \geq 0$. *Then, the model solutions (S(t),E(t),I(t),T(t),R(t)) are positive for* $t \geq 0$.

Proof. The lemma shall be proved via a contradiction knowing fully that $N(t) \neq 0$ for all $t \geq 0$. Assuming there exists the times, $(t_1, t_2, t_3, t_4, t_5)$ such that for $S(t) > 0$, $S(t_1) = 0$ is assumed. Then,

$$\frac{dS(t_1)}{dt} < 0, E(0) \geq 0, I(0) \geq 0, T(0) \geq 0, R(0) \geq 0, 0 \leq t \leq t_1.$$

$$\therefore \frac{dS(t_1)}{dt} < 0 \Rightarrow \frac{dS(t_1)}{dt}|_{t=t_1} = p - (\epsilon_I \beta I + \epsilon_E \beta E + \epsilon_T \beta T + \mu) S(t_1) = p \leq 0,$$

which is a contradiction since $p > 0$. Therefore, it follows that $S(t) \geq 0, \forall\, t \geq 0$.

For $E(t) > 0$: Suppose $E(t_2) = 0$, $\frac{dE(t_2)}{dt} < 0, S(0) \geq 0, I(0) \geq 0, T(0) \geq 0, R(0) \geq 0, 0 \leq t \leq t_2$.

$$\begin{aligned} \frac{dE(t_2)}{dt} < 0 \Rightarrow \frac{dE(t_2)}{dt}|_{t=t_2} &= (\epsilon_I \beta I + \epsilon_E \beta E + \epsilon_T \beta T) S(t_2) - (\mu + \phi) E(t_2) \\ &= (\epsilon_I \beta I + \epsilon_E \beta E + \epsilon_T \beta T) S(t_2) \leq 0, \end{aligned}$$

a contradiction as well. Therefore, $E(t) \geq 0, \forall\, t \geq 0$.

For $I(t) > 0$: Assuming $I(t_3) = 0$, $\frac{dI(t_3)}{dt} < 0, S(0) \geq 0, E(0) \geq 0, T(0) \geq 0, R(0) \geq 0, 0 \leq t \leq t_3$.

$$\begin{aligned} \frac{dI(t_3)}{dt} < 0 \Rightarrow \frac{dI(t_3)}{dt}|_{t=t_3} &= (1 - \alpha)\phi E(t_3) - (\mu + \rho + d_1) I(t_3) \\ &= (1 - \alpha)\phi E(t_3) \leq 0, \end{aligned}$$

a contradiction which implies that $I(t) \geq 0, \forall\, t \geq 0$.

For $T(t) > 0$: Suppose $T(t_4) = 0$, $\frac{dT(t_4)}{dt} < 0, S(0) \geq 0, E(0) \geq 0, I(0) \geq 0, R(0) \geq 0, 0 \leq t \leq t_4$.

$$\begin{aligned} \frac{dT(t_4)}{dt} < 0 \Rightarrow \frac{dT(t_4)}{dt}|_{t=t_4} &= \alpha\phi E(t_4) + \rho I(t_4) - (\mu + \tau + d_2) T(t_4) \\ &= \alpha\phi E(t_4) + \rho I(t_4) \leq 0, \end{aligned}$$

a contradiction since all the parameters are nonnegative. Therefore, $T(t) \geq 0, \forall\, t \geq 0$.

Lastly, for $R(t) > 0$: Suppose $R(t_5) = 0$, $\frac{dR(t_5)}{dt} < 0, S(0) \geq 0, E(0) \geq 0, I(0) \geq 0, T(0) \geq 0, 0 \leq t \leq t_5$.

$$\frac{dR(t_5)}{dt} < 0 \Rightarrow \frac{dT(t_5)}{dt}|_{t=t_5} = \tau T(t_5) - \mu R(t_5) = \tau T(t_5) \leq 0,$$

a contradiction since τ is nonnegative. Hence, $R(t) \geq 0, \forall\, t \geq 0$. Consequently, the solutions $S(t), E(t), I(t), T(t)$ and $R(t)$ remain nonnegative for all $t > 0$. □

3. Equilibria and Stability

The model consists of two equilibria – zero and nonzero equilibria when the population is free from COVID-19 and when it is invaded with the virus respectively. The stability of the two equilibria is studied next.

3.1. **Stability Analysis of the Zero Equilibrium.** Zero equilibrium is obtained when the rate of change of all the compartments w.r.t. t, infection terms, infection compartments as well as recovered compartment are reduced to zero such that

$$N = S = S_0, S = S_0 = \frac{p}{\mu} \text{ and } E = I = T = R = 0.$$

After deriving the zero equilibrium, the parameter that governs the transmission potential of the disease, the reproduction number, is derived by following the approach in [14]. Two reproduction numbers are obtained - the basic reproduction number, $\mathcal{R}_0$, that governs the stability behaviour of the zero equilibrium and the control reproduction number, $\mathcal{R}_c$, that determines the stability of the nonzero equilibrium as in [18]. Let $\mathbf{x} = (E, I, T, R, S)^T$, such that

$$\frac{d\mathbf{x}}{dt} = \mathcal{F} - \mathcal{V}, \tag{3.1}$$

where

$$\mathcal{F} = ((\epsilon_I\beta I + \epsilon_E\beta E + \epsilon_T\beta T)S_0, 0, 0, 0, 0)^T$$

and,

$$\mathcal{V} = \begin{pmatrix} (\mu+\phi)E \\ -(1-\alpha)\phi E + (\mu+\rho+d_1)I \\ -\alpha\phi E - \rho I + (\mu+\tau+d_2)T \\ -\tau T + \mu R \\ -p + (\epsilon_I\beta I + \epsilon_E\beta E + \epsilon_T\beta T)S_0 + \mu S_0 \end{pmatrix}$$

The matrices F and V are derived by considering only the infective compartments and

$$F = \begin{pmatrix} \epsilon_E\beta S_0 & \epsilon_I\beta S_0 & \epsilon_T\beta S_0 \\ 0 & 0 & 0 \\ 0 & 0 & 0 \end{pmatrix}, \tag{3.2}$$

$$V = \begin{pmatrix} (\mu+\phi) & 0 & 0 \\ -(1-\alpha)\phi & (\mu+\rho+d_1) & 0 \\ -\alpha\phi & -\rho & (\mu+\tau+d_2) \end{pmatrix}. \tag{3.3}$$

The inverse of V is obtained as

$$\mathcal{V}^{-1} = \begin{pmatrix} \frac{1}{(\mu+\phi)} & 0 & 0 \\ \frac{(1-\alpha)\phi}{(\mu+\phi)(\mu+\rho+d_1)} & \frac{1}{(\mu+\rho+d_1)} & 0 \\ \frac{\rho(1-\alpha)\phi + (\mu+\rho+d_1)\alpha\phi}{(\mu+\phi)(\mu+\rho+d_1)(\mu+\tau+d_2)} & \frac{\rho}{(\mu+\rho+d_1)(\mu+\tau+d_2)} & \frac{1}{(\mu+\tau+d_2)} \end{pmatrix} \tag{3.4}$$

and, the product of F and V^{-1} is obtained as

$$FV^{-1} = \begin{pmatrix} \frac{\epsilon_E\beta S_0}{k_1} + \frac{\epsilon_I\beta(1-\alpha)\phi S_0}{k_1k_2} + \frac{\epsilon_T\beta k_4 S_0}{k_1k_2k_3} & \frac{\epsilon_I\beta S_0}{k_2} + \frac{\epsilon_T\beta\rho S_0}{k_2k_3} & \frac{\epsilon_T\beta S_0}{k_3} \\ 0 & 0 & 0 \\ 0 & 0 & 0 \end{pmatrix} \tag{3.5}$$

where

$$k_1 = \mu+\phi, k_2 = \mu+\rho+d_1, k_3 = \mu+\tau+d_2, \text{ and } k_4 = \rho(1-\alpha)\phi + (\mu+\rho+d_1)\alpha\phi.$$

The eigenvalues of Eq.(3.5) are:
$\lambda_1 = \frac{\epsilon_E\beta S_0}{k_1} + \frac{\epsilon_I\beta(1-\alpha)\phi S_0}{k_1k_2} + \frac{\epsilon_T\beta k_4 S_0}{k_1k_2k_3}, \lambda_2 = \lambda_3 = 0$ and the control reproduction number, $\mathcal{R}_c$, is the largest eigenvalue.

$$\therefore \mathcal{R}_c = \lambda_1 = \frac{\epsilon_E\beta S_0}{k_1} + \frac{\epsilon_I\beta(1-\alpha)\phi S_0}{k_1k_2} + \frac{\epsilon_T\beta k_4 S_0}{k_1k_2k_3}. \tag{3.6}$$

Generally, when control measures are not on ground, disease transmission is discussed in terms of the basic reproduction number, which in the present analysis means $\rho = \alpha = 0$. Therefore, $\mathcal{R}_0$ is derived from $\mathcal{R}_c$ by setting $\rho = \alpha = 0$ and

$$\mathcal{R}_0 = \frac{\epsilon_E\beta S_0}{k_1} + \frac{\epsilon_I\beta\phi S_0}{k_1k_2}. \tag{3.7}$$

The two results in Eqs.(3.6) and (3.7) are crucial and are used to investigate the stability of the nonzero and zero equilibria respectively as in [18]. When $\rho = \alpha = 0$, there is no new infections that enter treatment class. However, treatment class cannot be empty since the analysis is around the origin which implies that some individuals might have been infected and isolated for treatment initially.

Theorem 1. *The zero equilibrium of the model is locally asymptotically stable if $\mathcal{R}_c < 1$ but is unstable if $\mathcal{R}_c > 1$.*

Proof. The variational matrix of the system evaluated at the zero equilibrium, $\mathcal{W}_0 = \left(\frac{p}{\mu}, 0, 0, 0, 0\right)$ is given by

$$J(\mathcal{W}_0) = \begin{pmatrix} -\mu & -\epsilon_E\beta S_0 & -\epsilon_I\beta S_0 & -\epsilon_T\beta S_0 & 0 \\ 0 & -(\mu+\phi)+\epsilon_E\beta S_0 & \epsilon_I\beta S_0 & \epsilon_T\beta S_0 & 0 \\ 0 & (1-\alpha)\phi & -(\mu+\rho+d_1) & 0 & 0 \\ 0 & \alpha\phi & \rho & -(\mu+\tau+d_1) & 0 \\ 0 & 0 & 0 & \tau & -\mu \end{pmatrix} \tag{3.8}$$

The matrix in Eq.(3.8) has double negative eigenvalues (i.e. -μ). The three other eigenvalues can be obtained from sub matrix $\mathcal{A}$, given as

$$\mathcal{A} = \begin{pmatrix} -(\mu+\phi)+\epsilon_E\beta S_0 & \epsilon_I\beta S_0 & \epsilon_T\beta S_0 \\ (1-\alpha)\phi & -(\mu+\rho+d_1) & 0 \\ \alpha\phi & \rho & -(\mu+\tau+d_2) \end{pmatrix} \tag{3.9}$$

In Eq.(3.9),

$$tr(\mathcal{A}) = -(\phi+\rho+\tau+3\mu+d_1+d_2)+\epsilon_E\beta S_0, \tag{3.10}$$

and,

$$\begin{aligned} det(\mathcal{A}) = {} & (\mu+\rho+d_1)(\mu+\tau+d_2)(\epsilon_E\beta S_0-\mu-\phi)+\epsilon_I\beta S_0(\mu+\tau+d_2)(1-\alpha)\phi \\ & +\epsilon_T\beta S_0(\rho(1-\alpha)+\alpha\phi(\mu+\rho+d_1)). \end{aligned} \tag{3.11}$$

The remaining eigenvalues of the Jacobian matrix $J(\mathcal{W}_0)$ are all negative if $tr(\mathcal{A}) < 0$ and $det(\mathcal{A}) > 0$. Therefore, $\mathcal{R}_c < 1$ and zero equilibrium $\mathcal{W}_0$ is locally asymptotically stable if $tr(\mathcal{A}) < 0$ and $det(\mathcal{A}) > 0$. If any of the conditions $tr(\mathcal{A}) < 0$ or $det(\mathcal{A}) > 0$ is not satisfied then $\mathcal{R}_c > 1$ and zero equilibrium $\mathcal{W}_0$ is unstable. □

3.2. **Existence and Stability of Nonzero Equilibrium.** Nonzero equilibrium exists when the population is invaded with the virus such that each compartment is nonempty. Given the force of infection as

$$\lambda^* = \epsilon_E\beta E^* + \epsilon_I\beta I^* + \epsilon_T\beta T^* \tag{3.12}$$

The population in each compartment is obtained when Eqs.(2.2)-(2.6) are set to zero and solved such that

$$S^* = \frac{p}{\mu + \lambda^*}, \tag{3.13}$$

$$E^* = \frac{p\lambda^*}{(\mu + \lambda^*)(\mu + \phi)}, \tag{3.14}$$

$$I^* = \frac{(1-\alpha)\phi}{(\mu + \rho + d_1)} E^*, \tag{3.15}$$

$$T^* = \frac{[\alpha\phi(\mu + \rho + d_1) + \rho(1-\alpha)\phi]E^*}{(\mu + \rho + d_1)(\mu + \tau + d_2)}, \tag{3.16}$$

$$R^* = \frac{\tau[\alpha\phi(\mu + \rho + d_1) + \rho(1-\alpha)\phi]E^*}{\mu(\mu + \rho + d_1)(\mu + \tau + d_2)}. \tag{3.17}$$

Putting Eqs.(3.13)-(3.17) into Eq.(3.12), reduces to

$$(\lambda^*)^2 + \lambda^* \left[\mu - p\left\{\frac{\epsilon_E \beta S_0}{k_1} + \frac{\epsilon_I \beta(1-\alpha)\phi S_0}{k_1 k_2} + \frac{\epsilon_T \beta k_4 S_0}{k_1 k_2 k_3}\right\}\right] = 0, \tag{3.18}$$

where

$$k_1 = \mu + \phi, k_2 = \mu + \rho + d_1, k_3 = \mu + \tau + d_2, \text{ and } k_4 = \rho(1-\alpha)\phi + (\mu + \rho + d_1)\alpha\phi.$$

In view of Eq.(3.6), Eq.(3.18) becomes

$$\lambda^*[\lambda^* + \mu - p\mathcal{R}_c] = 0 \tag{3.19}$$

From Eq.(3.19), there exists two roots,

$$\lambda_1^* = 0 \text{ and } \lambda_2^* = \mu\left(\frac{p}{\mu}\mathcal{R}_c - 1\right).$$

The coordinates of the endemic equilibrium $W^* = (S^*, E^*, I^*, T^*, R^*)$ can therefore be derived by putting the result of λ_2^* into Eqs.(3.13)-(3.17) to obtain

$$\begin{aligned} S^* &= \frac{1}{\mathcal{R}_c}, \\ E^* &= \frac{p\mathcal{R}_c - \mu}{k_1\mathcal{R}_c}, \\ I^* &= \frac{(1-\alpha)\phi}{k_2}\left[\frac{p\mathcal{R}_c - \mu}{k_1\mathcal{R}_c}\right], \\ T^* &= \frac{k_4}{k_2 k_3}\left[\frac{p\mathcal{R}_c - \mu}{k_1\mathcal{R}_c}\right], \\ R^* &= \frac{\tau k_4}{\mu k_2 k_3}\left[\frac{p\mathcal{R}_c - \mu}{k_1\mathcal{R}_c}\right]. \end{aligned} \tag{3.20}$$

Theorem 2. *The zero equilibrium of the model is globally asymptotically stable if the time derivative of the Lyapunov function $\mathcal{V}$ is negative definite.*

Proof. Consider a time derivative Lyapunov function $\mathcal{V}$ defined as

$$\begin{aligned}
&\dot{\mathcal{V}} = A_1\dot{E} + A_2\dot{I} + A_3\dot{T} \text{ such that}\\
&\dot{\mathcal{V}} = A_1[(\epsilon_I\beta I + \epsilon_E\beta E + \epsilon_T\beta T)S - (\mu+\phi)E]\\
&\quad = +A_2[(1-\alpha)\phi E - (\mu+\rho+d_1)I] + A_3[\alpha\phi E + \rho I - (\mu+\tau+d_2)T],\\
&\Rightarrow\dot{\mathcal{V}} \leq (\epsilon_E\beta E + \epsilon_I\beta I + \epsilon_T\beta T)S - (\mu+\phi)E,\\
&\Rightarrow\dot{\mathcal{V}} \leq (\mu+\phi)\left[\frac{\epsilon_E\beta S_0}{k_1} + \frac{\epsilon_I\beta(1-\alpha)\phi S_0}{k_1k_2} + \frac{\epsilon_T\beta k_4 S_0}{k_1k_2k_3} - 1\right]E,\\
&\Rightarrow\dot{\mathcal{V}} \leq (\mu+\phi)[\mathcal{R}_c - 1]E
\end{aligned}$$

If $\mathcal{R}_c < 1$, the time derivative of the Lyapunov function is negative definite and the zero equilibrium of the model is globally asymptotically stable but if $\mathcal{R}_c > 1$, the zero equilibrium becomes unstable because $\dot{\mathcal{V}}$. □

Theorem 3. *The nonzero equilibrium $\mathcal{W}^*$ of the model is locally asymptotically stable if $\mathcal{R}_c > 1$.*

Proof. Assuming $S = x_1, E = x_2, I = x_3, T = x_4, R = x_5$ such that the model Eqs. (2.2)-(2.6) is rewritten as

$$\frac{dx}{dt} = f = (f_1, f_2, f_3, f_4, f_5),$$

where f is given as

$$\frac{dx_1}{dt} = f_1 = p - \beta^*(\epsilon_E x_2 + \epsilon_I x_3 + \epsilon_T x_4)x_1 - \mu x_1, \tag{3.21}$$

$$\frac{dx_2}{dt} = f_2 = \beta^*(\epsilon_E x_2 + \epsilon_I x_3 + \epsilon_T x_4)x_1 - k_1 x_2, \tag{3.22}$$

$$\frac{dx_3}{dt} = f_3 = (1-\alpha)\phi x_2 - k_2 x_3, \tag{3.23}$$

$$\frac{dx_4}{dt} = f_4 = \alpha\phi x_2 + \rho x_3 - k_3 x_4, \tag{3.24}$$

$$\frac{dx_5}{dt} = f_5 = \tau x_4 - \mu x_5 \tag{3.25}$$

The variational matrix of Eqs. (3.21)-(3.25) evaluated at the zero equilibrium is obtained as

$$J^* = J(\mathcal{W}_0)|_{\beta=\beta^*} = \begin{pmatrix} -\mu & -\epsilon_E\beta^* S_0 & -\epsilon_I\beta^* S_0 & -\epsilon_T\beta^* S_0 & 0\\ 0 & -k_1 + \epsilon_E\beta^* S_0 & \epsilon_I\beta^* S_0 & \epsilon_T\beta^* S_0 & 0\\ 0 & -(1-\alpha)\phi & -k_2 & 0 & 0\\ 0 & \phi\alpha & \rho & -k_3 & 0\\ 0 & 0 & 0 & \tau & -\mu. \end{pmatrix} \tag{3.26}$$

Taking $\beta = \beta^*$ and $\mathcal{R}_c = 1$, as the bifurcation parameter and bifurcation point respectively. Expressing β^* in terms of other parameters when $\mathcal{R}_c = 1$ in Eq.(3.6) then,

$$\beta^* = \frac{k_1k_2k_3}{k_2k_3\epsilon_E S_0 + k_3\epsilon_I(1-\alpha)\phi S_0 + \epsilon_T k_4 S_0} \tag{3.27}$$

The centre manifold theory in [13] can be used to analyse the local asymptotic stability of the nonzero equilibrium of the model Eqs. (3.21)-(3.25) in the neighborhood of $\beta = \beta^*$ The right eigen vector of the variational matrix

$J(\mathcal{W}_0)|_{\beta=\beta^*}$ in terms of $w_2 > 0$ is obtained as

$$w_1 = -\frac{\beta^* S_0[k_3(k_2\epsilon_E + \epsilon_I(1-\alpha)\phi) + \epsilon_T k_4]}{\mu k_2 k_3} w_2, \tag{3.28}$$

$$w_2 = w_2 > 0, \tag{3.29}$$

$$w_3 = \frac{(1-\alpha)\phi}{k_2} w_2 > 0, \tag{3.30}$$

$$w_4 = \frac{k_4}{k_2 k_3} w_2 > 0, \tag{3.31}$$

$$w_5 = \frac{\tau k_4}{\mu k_2 k_3} w_2 > 0. \tag{3.32}$$

Also, the left-eigenvector of the variational matrix $J(\mathcal{W}_0)|_{\beta=\beta^*}$ at the zero equilibrium W_0 in terms of v_2 is obtained as

$$2v_2 w_1 w_2 \frac{\partial^2 f_2}{\partial x_1 \partial x_2}(0,0) = 2v_2 w_1 w_2 \epsilon_E \beta^*, \tag{3.33}$$

$$2v_2 w_1 w_3 \frac{\partial^2 f_2}{\partial x_1 \partial x_3}(0,0) = 2v_2 w_1 w_3 \epsilon_I \beta^*, \tag{3.34}$$

$$2v_2 w_1 w_4 \frac{\partial^2 f_2}{\partial x_1 \partial x_4}(0,0) = 2v_2 w_1 w_4 \epsilon_T \beta^*. \tag{3.35}$$

Since the right and left eigenvector have been determined, the coefficients of bifurcation a and b are given by the article (iv) in [[13] Theorem 4.1] as

$$\begin{aligned} a &= \sum_{k,i,j=1}^{5} v_k w_i w_j \frac{\partial^2 f_k}{\partial x_i \partial x_j}(0,0), \\ &= 2v_2 w_1 \beta^* [w_2\epsilon_E + w_3\epsilon_I + \epsilon_T]. \end{aligned}$$

In Eqs. (3.28)-(3.32), $w_1 < 0$ but $w_2 > 0$, $w_3 > 0$, and $w_4 > 0$. Hence,

$$a = -2v_2 w_1 \beta^* [w_2\epsilon_E + w_3\epsilon_I + \epsilon_T] < 0 \tag{3.36}$$

and,

$$\begin{aligned} b &= \sum_{k,i=1}^{5} v_k w_i \frac{\partial^2 f_k}{\partial x_i \partial \beta_1^*}(0,0), \\ &= v_2 w_2 S_0. \end{aligned} \tag{3.37}$$

According to item (iv), Theorem 4.1 in [13] and the fact that $a < 0$ and $b > 0$ in Eqs.(3.36) and (3.37), it follows that the model has a unique nonzero equilibrium near $\mathcal{W}_0$ that is locally asymptotically stable if $\mathcal{R}_c > 1$. □

3.3. **Global Stability Analysis of the Non-Zero Equilibrium.** The analysis for the stability of the nonzero equilibrium becomes global when it is extended beyond the neighborhood of $\mathcal{W}_0$, the zero equilibrium. The following result for global stability of the nonzero equilibrium is therefore claimed.

Theorem 4. *The nonzero equilibrium of the system is globally asymptotically stable if $\mathcal{R}_c > 1$.*

Proof. The popular nonlinear Lyapunov function in [9, 40–42] shall be applied to verify the global stability of the nonzero equilibrium of the system.
Suppose

$$\begin{aligned} V(S,E,I,T,R) = S - S^* + c_1(E - E^* \ln E) + c_2(I - I^* \ln I) \\ + c_3(T - T^* \ln T) + c_4(R - R^* \ln R), \end{aligned} \tag{3.38}$$

where c_1, c_2, c_3, c_4 are nonnegative Lyapunov constants.
Eq.(3.38) satisfies

$$\frac{dV}{dt} = \frac{\partial V}{\partial S}\frac{dS}{dt} + \frac{\partial V}{\partial E}\frac{dE}{dt} + \frac{\partial V}{\partial I}\frac{dI}{dt} + \frac{\partial V}{\partial T}\frac{dT}{dt} + \frac{\partial V}{\partial R}\frac{dR}{dt},$$

which becomes

$$\begin{aligned}
\dot{V}(S,E,I,T,R) &= \left(1-\frac{S^*}{S}\right)\dot{S} + c_1\left(1-\frac{E^*}{E}\right)\dot{E} + c_2\left(1-\frac{I^*}{I}\right)\dot{I} \\
&+ c_3\left(1-\frac{I^*}{I}\right)\dot{I} + c_4\left(1-\frac{R^*}{R}\right)\dot{R} \\
&= \left(1-\frac{S^*}{S}\right)[p-(\epsilon_I\beta IS + \epsilon_E\beta ES + \epsilon_T\beta TS + \mu S)] \\
&+ c_1\left(1-\frac{E^*}{E}\right)[\epsilon_I\beta IS + \epsilon_E\beta ES + \epsilon_T\beta TS - (\mu+\phi)E] \\
&+ c_2\left(1-\frac{I^*}{I}\right)[(1-\alpha)\phi E - (\mu+\rho+d_1)I] \\
&+ c_3\left(1-\frac{T^*}{T}\right)[\alpha\phi E + \rho I - (\mu+\tau+d_2)T] \\
&+ c_4\left(1-\frac{R^*}{R}\right)[\tau T - \mu R].
\end{aligned} \tag{3.39}$$

At endemic equilibrium, the system (2.2)-(2.6) can be written as

$$\begin{aligned}
p &= \epsilon_I\beta I^*S^* + \epsilon_E\beta E^*S^* + \epsilon_T\beta T^*S^* + \mu S^*, \\
(\mu+\phi) &= \frac{\epsilon_I\beta I^*S^* + \epsilon_E\beta E^*S^* + \epsilon_T\beta T^*S^*}{E^*}, \\
(\mu+\rho+d_1) &= \frac{(1-\alpha)\phi}{I^*}, \\
(\mu+\tau+d_2) &= \frac{\alpha\phi E^* + \rho I^*}{T^*}, \\
\mu &= \frac{\tau T^*}{R^*}.
\end{aligned}$$

Appropriate substitution of the values of $p, (\mu+\phi), (\mu+\rho+d_1), (\mu+\tau+d_2)$ and μ into Eq.(3.39) and ample simplification gives

$$\begin{aligned}
\dot{V}(S,E,I,T,R) &= \mu S^*\left(2 - \frac{S}{S^*} - \frac{S^*}{S}\right) + A_1\left(1-\frac{S^*}{S}\right) + A_2\left(1-\frac{S}{S^*}\right) \\
&+ A_3\left(1-\frac{E^*}{E}\right) + A_4\left(1-\frac{E}{E^*}\right) + A_5\left(1-\frac{I^*}{I}\right) \\
&+ A_6\left(1-\frac{I}{I^*}\right) + A_7\left(1-\frac{T^*}{T}\right) + A_8\left(1-\frac{T}{T^*}\right) \\
&+ A_9\left(1-\frac{R^*}{R}\right) + A_{10}\left(1-\frac{R}{R^*}\right),
\end{aligned} \tag{3.40}$$

where $A_1, \cdots, A_{10}$ are nonnegative constants.
Since arithmetic mean exceeds geometric mean [23, 43], $\left(2 - \frac{S}{S^*} - \frac{S^*}{S}\right) \leq 0$. Also, since $\mathcal{W}^* = (S^*, E^*, I^*, T^*, R^*)$ is a point in $\mathcal{W}_0 = (S_0, E_0, I_0, T_0, R_0)$ then

$\left(1-\frac{S^*}{S}\right)>0, \left(1-\frac{E^*}{E}\right)>0, \left(1-\frac{I^*}{I}\right)>0, \left(1-\frac{T^*}{T}\right)>0$ and $\left(1-\frac{R^*}{R}\right)>0$ but $\left(1-\frac{S}{S^*}\right)<0, \left(1-\frac{E}{E^*}\right)<0, \left(1-\frac{I}{I^*}\right)<0, \left(1-\frac{T}{T^*}\right)<0$ and $\left(1-\frac{R}{R^*}\right)<0$. One can therefore see from Eq.(3.40) that $\dot{V}$ consists of both positive and negative terms. Suppose $\dot{V}$ is written in terms of B_1 and B_2 where B_1 denotes all the positive terms and B_2, all the negative terms then $\dot{V}=B_1+B_2$. Hence, $\dot{V}<0$ if $B_1<B_2$. Also, $\dot{V}=0$ provided that $S^*=S, E^*=E, I^*=I, T^*=T$ and $R^*=R$. The singleton $\mathcal{W}^*$ is therefore the largest compact invariant set in $[(S,E,I,T,R)\in\Omega:\dot{V}=0,]$ where $\mathcal{W}^*$ is the endemic equilibrium. It is therefore follows from LaSalle invariance principle [27] that $\mathcal{W}^*$ is globally asymptotically stable in the interior Ω. □

3.4. **Sensitivity Analysis.** The relative importance of the key system parameters to the dynamics of the disease is derived analytically via the normalised forward sensitivity index formula in [7, 38, 44] thus

$$\frac{\partial\mathcal{R}_c}{\partial\beta}=\frac{\epsilon_E}{k_1}S_0+\frac{\epsilon_I(1-\alpha)\phi}{k_1k_2}S_0+\frac{\epsilon_Tk_4}{k_1k_2k_3}S_0\times\frac{\beta}{R_c}, \tag{3.41}$$

$$\frac{\partial\mathcal{R}_c}{\partial\epsilon_E}=\frac{\beta}{k_1}S_0\times\frac{\epsilon_E}{R_c}, \tag{3.42}$$

$$\frac{\partial\mathcal{R}_c}{\partial\epsilon_I}=\frac{\beta(1-\alpha)\phi}{k_1k_2}S_0\times\frac{\epsilon_I}{R_c}, \tag{3.43}$$

$$\frac{\partial\mathcal{R}_c}{\partial\epsilon_T}=\frac{\beta k_4}{k_1k_2k_3}S_0\times\frac{\epsilon_T}{R_c}, \tag{3.44}$$

$$\frac{\partial\mathcal{R}_c}{\partial\alpha}=-\phi\beta\frac{[\epsilon_Ik_3+\epsilon_T\rho]}{k_1k_2k_3}S_0\times\frac{\alpha}{R_c}, \tag{3.45}$$

$$\frac{\partial\mathcal{R}_c}{\partial\tau}=-\frac{\epsilon_T\beta k_4}{k_1k_2(k_3)^2}S_0\times\frac{\tau}{R_c}. \tag{3.46}$$

4. Results and Discussion

Numerical simulation is needed for the confirmation of the strength of theoretical results. Using parameter values in Table 1, the numerical values for the relative contributions of the major model parameters given in Eqs. (3.41)-(3.46) are computed in Table 2.

Table 2. Sensitivity indices of the major system parameters.

Parameters	Definitions
β	1.0000
ϵ_I	0.4167
ϵ_E	0.2194
ϵ_T	0.3639
α	-0.1268
τ	-0.2461

In Table 2, the most important parameter to COVID-19 transmission is the effective contact rate with infective agents while the most important parameter to COVID-19 management is the successful rate of treatment. Unprotected contacts with COVID-19 patients, particularly the asymptomatic individuals who spread the virus unintentionally, could escalate COVID-19 transmission while effective treatment could reduce the spread and deaths of COVID-19. Also, various enlightenment campaigns, particularly the encouragement of COVID-19 test, increased α, the proportion of infective who were detected and isolated for treatment at asymptomatic phase of infection. Therefore, parameter α was equally important in stemming the spread of COVID-19 and played significant roles in the control of COVID-19 pandemic. COVID-19 transmission could not be linear because individuals took various protective and

preventive measures against COVID-19 infections which brought about reduction factors ϵ_I, ϵ_E, and ϵ_T, the rate at which one prevented oneself from contracting COVID-19 from visibly infected individuals, all individuals generally and individuals who were under COVID-19 treatment respectively. Of all the three reduction factors, ϵ_I, the rate at which one prevented oneself from contracting COVID-19 from visibly infected individuals, is the most sensitive factor. Therefore, the extent at which people keep away from the visibly infected COVID-19 patients contributed immeasurably to COVID-19 spread minimization during the pandemic. Now, to observe the effects of the control parameters α, ρ and τ on the dynamics of COVID-19, we carry out simulations by using different values of these parameters and the results are displayed in Figures 2 - 5.

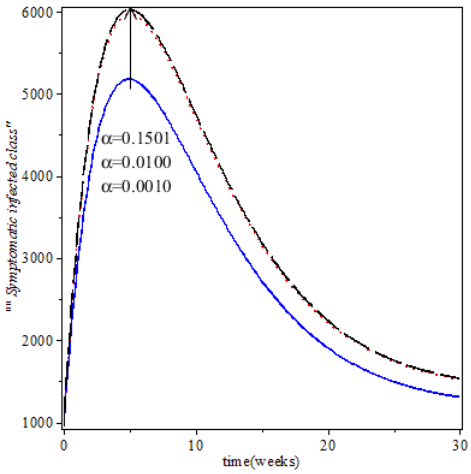

(A) Effect of decrease in α on the population of symptomatic individuals.

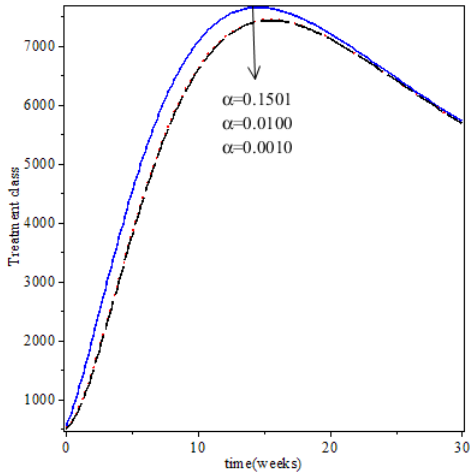

(B) Effect of decrease in α on the population of individuals under COVID-19 treatment.

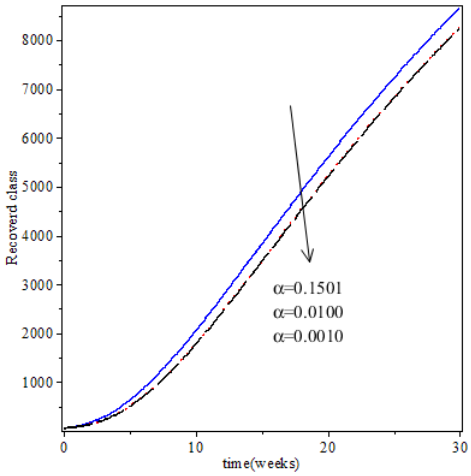

(C) Effect of decrease in α on the population of recovered individuals.

FIGURE 2. Simulation showing the effects of poor isolation of asymptomatic individuals on the dynamics of COVID-19.

Figure 2, shows the dynamics of the system with changes in the values of the control parameter α. Attention is focused on α because asymptomatic infectious individuals have the greatest tendency to spread the infections. The

impact of these set of people on disease propagation might be taken flippantly since they look healthy and show no symptoms of infections. We can observe from Figure 2a that when interventions were not put on ground to detect and isolate individuals who were asymptomatic to COVID-19, people became symptomatic freely and the population of symptomatic individuals jumped up and reached the peak before it began to drop. Although the populations of individuals in the treatment and recovered classes in Figures 2b and 2c increased continuously, the increases were at a decreasing rate owing to the inability to stem the infection at the asymptomatic phase. Generally, Figure 2 depicts COVID-19 dynamics at the start of the pandemic when some epidemiological features of the disease (e.g. infectivity, serial interval, incubation period, asymptomatics, etc.) were not known. At the beginning of the pandemic, the infection spread like the harmattan fire.

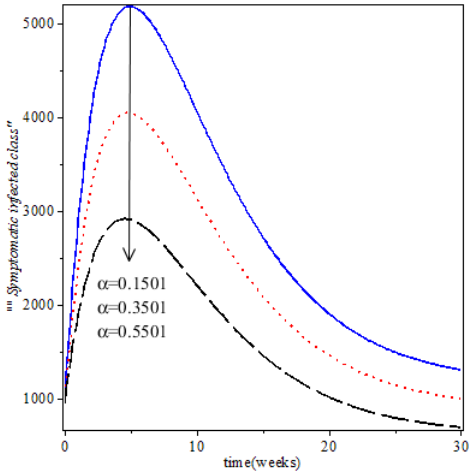

(A) Effect of increase in α on the population of symptomatic individuals.

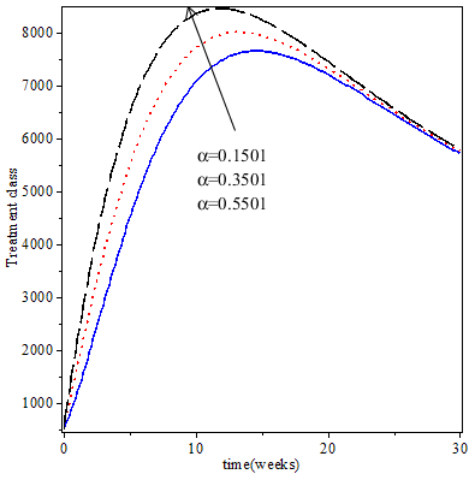

(B) Effect of increase in α on the population of individuals under COVID-19 treatment.

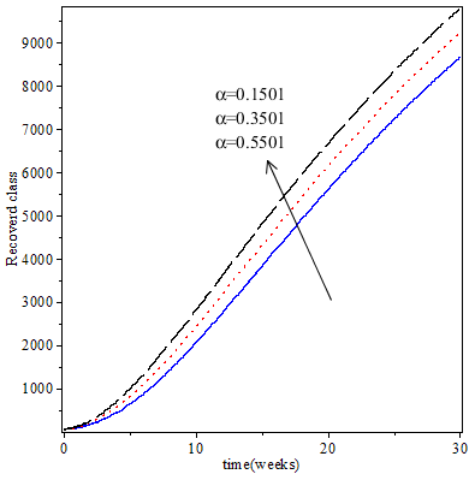

(C) Effect of increase in α on the population of recovered individuals.

FIGURE 3. Simulation showing the effects of prompt isolation of asymptomatic individuals on the dynamics of COVID-19.

The impacts of various strategies (e.g. testing, contact tracing, etc.) to discover COVID-19 infection at the asymptomatic phase are revealed in Figure 3. We observe in Figure 3a that as α increases, the number of individuals who are symptomatic to COVID-19 falls continuously and go to extinction after 30 weeks. The impacts of these strategies also increase the populations of individuals in treatment and recovered classes as shown in Figures 3b and 3c respectively. The behaviour of the model in Figure 3 described COVID-19 dynamics when the features of the virus were fully understood and the people were encouraged to start undergoing COVID-19 tests. Through the tests, many people who harboured the virus without showing symptoms were discovered and placed under treatments which eventually decreased the spread of the virus but increased the number of people who were under treatment and those who recovered from the virus.

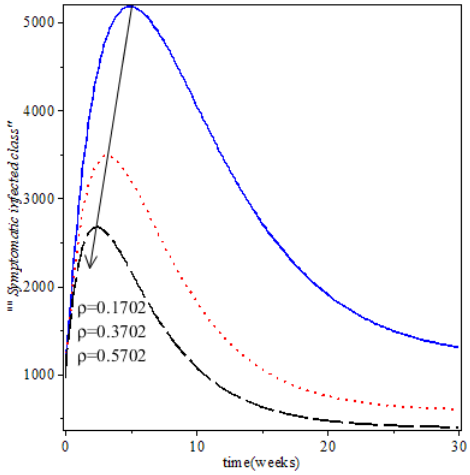

(A) Effect of increase in ρ on the population of symptomatic individuals.

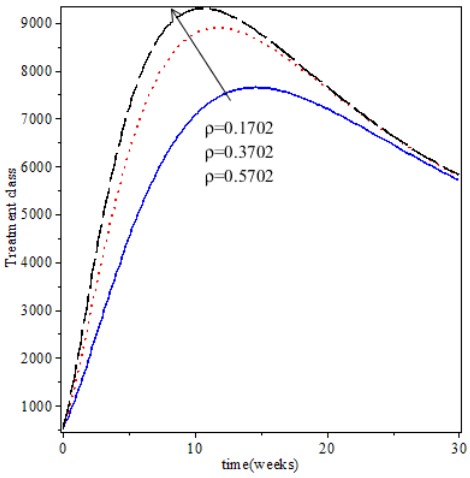

(B) Effect of increase in ρ on the population of individuals under COVID-19 treatment.

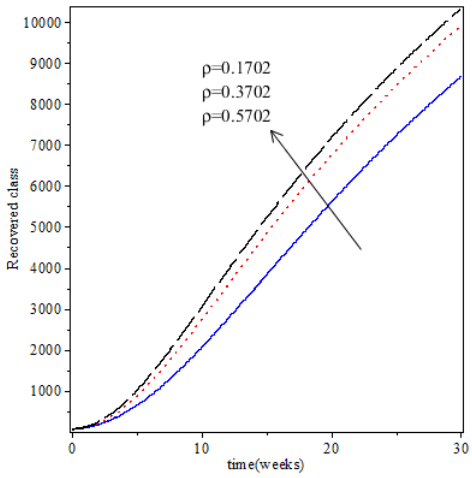

(C) Effect of increase in ρ on the population of recovered individuals.

FIGURE 4. Simulation showing the effects of isolation of symptomatic individuals on the dynamics of COVID-19.

Visibly infected individuals would seek medical attention without delay and this is revealed in Figure 4. As more and more COVID-19 visibly infected individuals seek medical attentions, the population of symptomatic individuals falls while the the number of people who are under treatments rises as indicated in Figures 4a and 4b respectively. Improved treatment lead to quick recovery which is indicated by increase in the number of recovered individuals in Figure 4c.

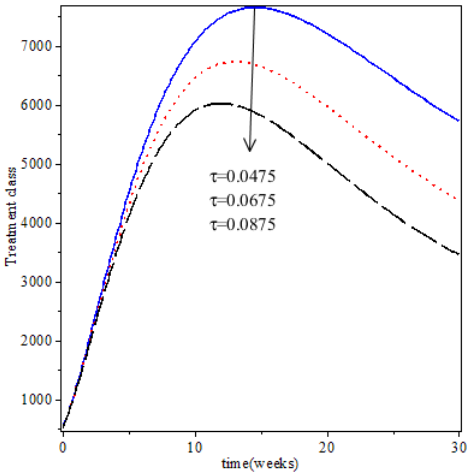

(A) Effect of increase in τ on the population of individuals under treatment.

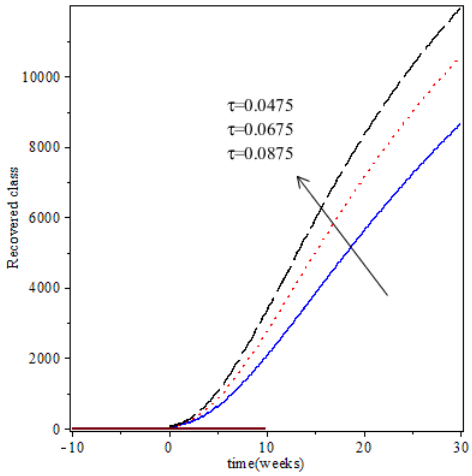

(B) Effect of increase in τ on the population of recovered individuals.

FIGURE 5. Simulation showing the effects of successful treatment on the dynamics of COVID-19.

A good number of individuals who were infected with COVID-19 were successfully treated when the pandemic was hot. Successful treatment of COVID-19 infections reduces the case fatality ratio (CFR) of the disease. The CFR of COVID-19 as of 1 October 2020 was 2.98 [4, 45]. That is, a ratio of 1,019,242 deaths to 34,192,734 reported cases. The massive reduction in COVID-19 CFR is attributable to successful treatment of the disease. The effect of treatment on the COVID-19 dynamics can be visualised in Figure 5 where an increase in the treatment parameter results in a decrease in the population of people who are under treatment (Figure 5a) but an increase in the population of recovered individuals (Figure 5b).

5. Conclusion

Isolation and quarantine are two epidemiological terms that have different interpretations. The present paper analysed the role played by isolation particularly at the asymptomatic phase of infection on the dynamics of COVID-19 pandemic via a compartmental model of a system of first-order nonlinear ordinary differential equations. The model solutions were proved to be positive and bounded before it was subjected to a rigorous qualitative analysis. The reproduction numbers were derived and used to investigate the local and global stability of the zero and nonzero equilibria. The necessary and sufficient conditions required by the zero and nonzero equilibria of the model to be locally and globally asymptotically stable were derived. The relative importance of the model parameters to disease spread and management was also studied and the contributions of some key model parameters to disease dynamics were derived analytically. Numerical simulation was conducted and it was established that the most sensitive parameter to COVID-19 transmission was effective contact rate while the most important parameter to COVID-19 management was successful treatment rate. Numerical simulation also revealed that COVID-19 incidence and prevalence depended majorly on the per capita probability of detecting infection at the asymptomatic phase. It was therefore realised from the simulation that isolation, which is aided by contact tracing and testing, played significant roles in the management of the COVID-19 when the pandemic was hot.

References

[1] Y. Althobaity and M. J. Tildesley, *Modelling the impact of non-pharmaceutical interventions on the spread of COVID-19 in Saudi Arabia*, Sci Rep., *13*(1) (2023), 843. doi: 10.1038/s41598-022-26468-5

[2] I. Asian, M. Demir, M. G. Wise, and S. Lenhart, *Modeling COVID-19: forecasting and analysing the dynamics of the outbreak in Hubei and Turkey*, Mathematical Methods in the Applied Sciences, *45*(10) (2022), 6481–6494.

[3] A. Atangana, *Modeling the spread of COVID-19 with new fractal-fractional operators: can the lockdown save mankind before vaccination?*, Chaos, Soliton& Fractals, *136* (2020), 109860.

[4] A. A. Ayoade, T. Latunde, and R. O. Folaranmi, *Comparative analysis of transmissibility and case fatality ratio of SARS, MERS and COVID-19 via a mathematical modeling approach*, Journal of Fundamental and Applied Sciences, *13*(3) (2021), 1262-1274.

[5] A. A. Ayoade, S. O. Agboola, and M. O. Ibrahim, *Mathematical analysis of the effect of maternal immunity on the global eradication of measles*, Annals.Computer Science Series, *17*(1) (2019), 235-241.

[6] A. A. Ayoade, O. Odetunde, and B. Falodun, *Modeling and analysis of the impact of vocational education on the unemployment rate in Nigeria*, Application and Applied Mathematics: An International Journal (AAM), *15* (2020), 550-564.

[7] A. A. Ayoade and O. Aliu, *COVID-19 outbreak and mitigation by movement restrictions: a mathematical assessment of economic impact on Nigerian households*, Journal of Quality Measurement and Analysis, *18*(2) (2022), 29-44.

[8] A. A. Ayoade and M. O. Ibrahim, *Analyis of transmission dynamics and mitigation success of COVID-19 in Nigeria: An insight from a mathematical model*, The Aligarh Bulletin of Mathematics, *41*(1) (2022), 1-26.

[9] B. Buonomo and C. Vargas-De-Leone, *Stability and bifurcation analysis of a vector-bias model of malaria transmission*, Mathematical Biosciences, *242* (2013), 59-72.

[10] Centre for Disease Prevention Control (CDC) *Human Coronavirus Types. National Centre for Immunisation and Respiratory Diseases (NCIRD), Division of Viral Diseases*, (2020). https://www.cdc.gov/coronavirus/types.html [accessed 15 May 2020].

[11] Z. Cakir and H. B. Savas, *A mathematical modeling approach in the spread of the novel 2019 coronavirus SARS-CoV-2 (COVID-19) pandemic*, Electronic Journal General Medicine, (2020). https://doi.org/10.29333/ejgm/78612224-2236

[12] CNN, *Coronavirus news: The novel coronavirus has infected over 118 000 and killed almost 4 300 worldwide*, (2020). https//www.cnn.com/world/live-news/coronavirus-outbreak-03-11-20-intl-hnk/index.html tr [accessed 26 July 2020].

[13] C. Castillo-Chavez and B. Song, *Dynamical models of tuberculosis and their applications*, Mathematical Biosciences and Engineering, *1* (2004), 361–404.

[14] P. V. D. Driessche and J. Watmough, *Reproduction number and sub – threshold endemic equilibria for compartmental models of disease transmission*, Mathematical Biosciences, *180* (2002), 29 – 48.

[15] A. O. Egonmwan and D. Okuonghae, *Mathematical analysis of a tuberculosis model with imperfect vaccin*, International Journal Biomathematics, *12* (2019), 1950073.

[16] S. E. Eikenberry, M. Mancuso, E. Iboi, T. Phan, E. Kostelich, Y. Kuang, and A. B. Gumel, *To mask or not to mask: Modelling the potential for face mask use by the general public to curtail the COVID-19 pandemic*, Infectious Disease Modelling, *5* (2020), 293–08.

[17] N. M. Ferguson, D. Laydon, G. Nedjati-Gilani, N. Imai, K. Ainslie, M. Baguelin, S. Bhatia, A. Boonyasiri, Z. Cucunuba, G. Cuomo-Dannenburg, G. et al. *Impact of non-pharmaceutical interventions (NPIs) to reduce COVID-19 mortality and healthcare demand*, Imperial College COVID-19 Response Team, London, Vol. 16, March, (2020).

[18] A. B. Gumel, S. Ruan, T. Day, J. Watmough, F. Brauer, P. V. D. Driessche, D. Gabrielson, C. Bowman, M. E. Alexander, S. Ardal, J. Wu, and B. M. Sahai, *Modelling strategies for controlling SARS outbreaks*, Proceeding of Royal Society of London (SeriesB), (2004). http://dx.doi.org/10.1098/rspb.2004.2800

[19] J. Hellewell, S. Abbott, A. Gimma, N. I. Bosse, C. I. Jarvis, T. W. Russell, J. D. Munday, A. J. Kucharski, W. J. Edmunds, F. Sun, et al. *Feasibility of controlling COVID-19 outbreaks by isolation of cases and contacts*, The

Lancet Global Health, (2020).
[20] E. Iboi, O. O. Sharomi, C. Ngonghala, and A. B. Gumel, *Mathematical modelling and analysis of COVID-19 pandemic in Nigeria*, Mathematical Biosciences and Engineering, *17*(6) (2020), 7192-7220.
[21] B. Ivorra, M. R. Ferrndez, M. Vela-Prez, and A. M. Ramos, *Mathematical modelling of the spread of the coronavirus disease 2019 (COVID-19) considering its particular characteristics. The case of China*, Communication in Nonlinear Science and Numerical Simulation, (2020). https://doi.org/10.1016/j.cnsns.2020.10530.
[22] J. M. Jorge M. Mendes and P. S. Coelho, *The effect of non-pharmaceutical interventions on COVID-19 outcomes: A heterogeneous age-related generalisation of the SEIR model*, Infectious Disease Modelling, *8*(2023), 742-768.
[23] O. A. S. Karamzadeh, *One-line proof of the AM-GM inequality*, Mathematical Intelligence, *33*(2) (2011). http://dx.doi.org/10.1007/s00283-010-9197-9
[24] W. O. Kermack and A. G. McKendrick, *A contribution to the mathematical theory of epidemics*, Proceeding of Royal Society of London (Series A), *115* (1927), 700–721.
[25] M. A. Khan, and A. Atangana, *Modelling the dynamics of novel coronavirus 2019-nCoV with fractional derivative*, Alexandra England. Journal,(2020). https://doi.org/10.1016/j.aej.2020.02.033.
[26] A. J. Kucharski, T. W. Russell, C. Diamond, Y. Liu, J. Edmunds, S. Funk, R. M. Eggo, F. Sun, M. Jit, J. D. Munday, et al. *Early dynamics of transmission and control of COVID-19: a mathematical modelling study*, The Lancet Infectious Diseases, (2020).
[27] J. P. LaSalle, *Stability theory for ordinary differential equations*, Journal of differential equations, *4* (1968), 57-65.
[28] Y. Liu, A. A. Gayle, A. Wilder-Smith, and A. Rocklv, *The reproductive number of COVID-19 is higher compared to SARS coronavirus*, Journal of Travel Medicine, (2020). doi: 10.1093/jtm/taaa021
[29] T. Mabuka, N. Ncube, M. Ross, A. Silaji, W. Macharia, T. Ndemara, and T. Lemeke, *The impact of non-pharmaceutical interventions on the first COVID-19 epidemic wave in South Africa*, BMC Public Health volume *23* (2023), Article number: 1492.
[30] A. Madhusudanan, C. Iddon, M. Cevik, J. H. Naismith, and S. Fitzgerald, *Non-pharmaceutical interventions for COVID-19: a systematic review on environmental control measures*, Philosophical Transactions of the Royal Society A Mathematical, Physical and Engineering, (2023). https://doi.org/10.1098/rsta.2023.0130
[31] K. Mizumoto and G. Chowell, *Transmission potential of the novel coronavirus (COVID-19) onboard the Diamond Princess Cruises Ship* , Infectious Disease Modelling, (2020).
[32] C. N. Ngonghala, E. Iboi, S. Eikenberry, M. Scotch, C. R. MacIntyre, M. H. Bonds, and A. B. Gumel, *Mathematical assessment of the impact of non-pharmaceutical interventions on curtailing the 2019 novel coronavirus*, Mathematical Biosciences, *325* (2020), 108364.
[33] A. Nwankwo and O. Okuonghae, *A mathematical model for the population dynamics of malaria with a temperature dependent control*, Differential Equation and Dynamical System, (2019). Doi:10.1007/s12591-019-00466-y.
[34] C. Ohia, A. S. Bakarey, and T. Ahmad, *COVID-19 and Nigeria: putting the reality in context*, International Journal of Infectious Disease, *95* (2020), 279-281.
[35] D. Okuonghae, *Backward bifurcation of an epidemiological model with saturated incidence, isolation and treatment function*, Qualitative Theory and Dynamical System, (2018) Doi:10.1007/s12346-018-0293-0.
[36] A. Omame, D. Okuonghae, R. A. Umana, and S. C. Inyama, *Analysis of a co-infection model for HPV-TB*, Applied Mathematical Model, *77* (2020), 881-901.
[37] A. Omame, D. Okuonghae, and S. C. Inyama, *A mathematical study of a model for HPV with two high risk strains*, Mathmatics applied to engineering, modeling and social issues, studies in systems, decision and control, *5* (2020), 33-44.
[38] H. S. Rodrigues, M. T. Monteiro, and D. F. M. Torres, *Sensitivity analysis in a dengue epidemiological model*, (2013). Retrieved December 13, 2020, from http://dx.doi.org/10.1155/2013/72140
[39] E. Shim, A. Tariq, W. Choi, Y. Lee, and G. Chowell, *Transmission potential and severity of COVID-19 in South Korea*, International Journal of Infectious Diseases, (2020).
[40] Z. Shuai and P. V. D. Driessche, *Global Stability of Infectious disease models using Lyapunov functions*, SIAM Journal of Applied Mathematics, *74* (2013), 1513 – 1532.

[41] S. Thota and A. A. Ayoade, *On dynamical analysis of a prey-diseased predator model with refuge in prey*, Applied Mathematics & Information Sciences, *15*(6) (2021), 717–721. doi: 10.18576/amis/150605.
[42] S. Thota, *A three species ecological model with Holling Type-II functional response*, Information Science Letters, *10*(3) (2021), 439–444. doi: 10.18576/isl/100307.
[43] S. Thota, *On an ecological model of mutualisim between two species with a mortal predator*, Applications and Applied Mathematics, *15*(2) (2020), 1309–1322.
[44] S. Thota, *A mathematical study on a diseased prey-predator model with predator harvesting*, Asian Journal of Fuzzy and Applied Mathematics, *8*(2) (2020), 16–21. https://doi.org/10.24203/ajfam.v8i2.6283
[45] S. Thota, *Prey-predator model for Awash National Park, Oromia, Ethiopia and its stability analysis with simulations*, Journal of Science and Sustainable Development, *7*(2) (2019), 15–21. DOI: https://doi.org/10.20372/au.jssd.7.2.2019.0133
[46] C. A. Whitfield, M. van Tongeren, Y. Han, H. Wei, S. Daniels, M. Regan, et. al. *Modelling the impact of non-pharmaceutical interventions on workplace transmission of SARS-CoV-2 in the home-delivery sector*, PLoS ONE, *18*(5) (2023), e0284805. https://doi.org/10.1371/journal.pone.0284805
[47] World Health Organisation (WHO), *Coronavirus*, (2020). WHO https://www.who.intl/health-topics/coronavirus [accessed 05 May 2020].